

Headline Articles

Effects of HMPA on the Structure and Reactivity of the Lithium Enolate of Cyclopentanone in THF: The Dimer is Responsible for Alkylation and Proton Exchange Reactions

Masaaki Suzuki,* Hiroko Koyama,[1] and Ryoji Noyori*,[1]

Division of Regeneration and Advanced Medical Science, Graduate School of Medicine, Gifu University, Yanagido, Gifu 501-1193

[1]Department of Chemistry and Research Center for Materials Science, Nagoya University, Chikusa, Nagoya 464-8602

Received August 20, 2003; E-mail: suzukims@biomol.gifu-u.ac.jp

The structure and reactivity of the lithium enolate of cyclopentanone are strongly influenced by coexisting HMPA molecules. Detailed low-temperature ^{7}Li, ^{31}P, and ^{13}C NMR studies of the 0.04–0.2 M THF solutions indicate that excess quantities of HMPA act primarily to form a bis-HMPA coordinated dimer. Tetrameric, trimeric, and monomeric enolates were not detected by HMPA titration. The convergency on the dimeric aggregate has been monitored by the successive displacement of THF with HMPA molecules. Even at a high concentration of HMPA, the formation of monomeric enolate was not observed. Kinetic experiments, combined with the structural information, showed that alkylation of the enolate by methyl iodide proceeds via the dimer with the assistance of HMPA. Proton exchange between the enolate and 2-methylcyclopentanone also occurs via the dimer, but without the participation of additional HMPA. These findings explain the role of HMPA in the selective monoalkylation of lithium enolate.

Lithium enolates are organic nucleophiles that are indispensable for the synthesis of many theoretically and practically important compounds.[1] Synthetic, structural, and kinetic studies over the past several decades have provided enormous progress in this chemistry.[1–5] Our interest in this subject stemmed from the three-component prostaglandin synthesis.[6] The key to our success was the modulation of the reactivity of a cyclopentanone enolate, generated in situ by conjugate addition of a lower side-chain organometallic to a protected 4-hydroxy-2-cyclopentenone **1** (Chart 1). Under certain controlled conditions, the regio-defined enolate can be trapped with an upper side-chain iodide, stereoselectively producing **2** without α-proton exchange; under these conditions, ketones also coexist in the reaction system.[6,7] The high selectivity for alkylation over proton exchange is crucial for the efficient vicinal carba-condensation of α,β-unsaturated ketones. When we investigated the behavior of a simple cyclopentanone enolate **3** in this reaction, we found that an HMPA additive had significant effects.[1,6c,d] The reaction of **3** with 5 molar amounts of methyl iodide in THF at 0 °C resulted in a 79% yield of 2-methylcyclopentanone (**4**), together with 15% polymethylated ketones (Scheme 1) that resulted from undesired enolate/ketone proton exchange reactions. The presence of 3 molar amounts of HMPA, however, significantly accelerated the alkylation at −78 °C to give a 94% yield of **4** accompanied by only 3.3% dimethylcyclopentanones (2,5/2,2 = 7).[6c] The main purpose of this study is the elucidation of the role of HMPA in this reaction system.[2e,8]

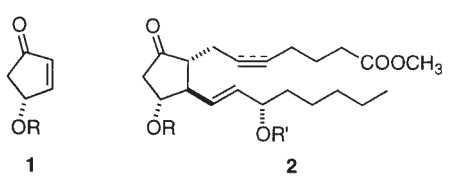

1 2

Chart 1.

The reactivity and selectivity of lithium enolates are profoundly influenced by the structures and reaction conditions, including particularly the solvents, the concentrations, and additives interacting with Li.[2–5,9–11] A milestone in this significant

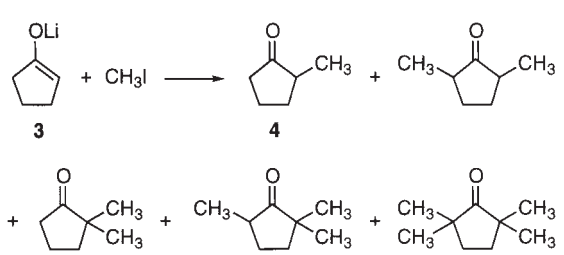

Scheme 1. Methylation of cyclopentanone lithium enolate by methyl iodide.

Published on the web February 10, 2004; DOI 10.1246/bcsj.77.259

subject was marked by Seebach,[3,4] who elucidated the X-ray structures of aggregates of lithium enolates crystallized with various solvents and ligands. This classic work implied the possibility of participation of these aggregates in the reactions of lithium enolates. Although Jackman[9] hypothesized that a tetrameric aggregate of the isobutyrophenone lithium enolate is directly involved in both the C- and O-alkylation reactions with dimethyl sulfate, which take place in a 0.16 M (1 M = 1 mol dm^{-3}) solution of 1,3-dioxolane or 1,2-dimethoxyethane, the actual structure of the reactive enolate remained unclear.[12]

To attempt to correlate reactivity with aggregation state, Streitwieser recently designed lithium enolates possessing a UV-detectable chromophore.[2] By performing detailed spectroscopic and rate studies in *dilute* THF solutions, they found that a monomeric lithium enolate equilibrating with its dimer or tetramer reacts with benzyl bromide in a concentration range of 6.2×10^{-4} M to 1.1×10^{-3} M.[2b,c] Moreover, an HMPA addend modulated the aggregation system, resulting in monomeric lithium enolates at a 10^{-4} M concentration, and the resulting monomers were observed to undergo further HMPA coordination to form a solvent-separated ion pair that participated in the alkylation.[2e]

NMR spectroscopy provides valuable information about the nature of lithium enolates in a higher concentration and about the equilibria in which they participate. Unlike lithium amides, which demonstrate $^{6/7}$Li–^{15}N coupling,[13] there have been few reports on lithium enolates,[5] due to the lack of Li–O coupling. Understanding this problem, Jackman cleverly used ^{13}C spin–lattice relaxation time and ^{7}Li quadrupole-splitting constants to analyze the structure of the enolate of isobutyrophenone, concluding that this enolate forms a tetrameric structure at a 10^{-1} M concentration.[5a] Furthermore, a study on lithium 3,5-dimethylphenolate as a model of lithium enolates, using ^{7}Li–^{31}P spin–spin long range coupling, $^{2}J(^{7}\text{Li}–^{31}\text{P})$,[14] showed that, in a 0.2 M ethereal solution containing 5 molar amounts of HMPA, the phenolate has an HMPA-coordinated tetrameric structure.[5c]

These findings suggested that the aggregation state of lithium enolates in solution is highly dependent on their organic backbones, intrinsic basicity and concentration, the steric factors of the coexisting solvent and other donor compounds, and the temperature of the reaction.[3,10,11] Obviously, each aggregate has a different nucleophilicity and basicity, resulting in complicated selectivity profiles.[15]

In this study, we demonstrate the participation of a dimeric enolate in an alkylation and proton exchange reaction. Using NMR, we have directly characterized the enolate responsible for this reaction. The role of HMPA was also clarified by both structural and kinetic methods. To our knowledge, this is the first such report showing the role of a dimeric enolate in this reaction.

Results and Discussion

Structures of Cyclopentanone Lithium Enolate in the Presence of HMPA. Enolate structures in ethereal solution are highly sensitive to their organic frameworks, whether cyclic or acyclic, sterically congested or uncongested, or electronically conjugated or nonconjugated.[3,10,11] In connection with our prostaglandin synthesis,[6] we had selected the lithium enolate **3**, which had been prepared by reaction of 1-(trimethylsiloxy)-cyclopentene and butyllithium.[16] While its THF solvate was observed to form a tetrameric structure possessing a Li_4O_4 cube in the crystalline state,[4] the melting-point depression measurement in 0.47 M THF solution at −107 °C suggested an average aggregation number of 2.8.[17] Thus, the addition of HMPA to the solution would be expected to result in its dissociation to a dimer with a Li_2O_2 square and, possibly, to a monomeric enolate[2e] having a contact or solvent-separated ion-paired structure.[5c,14b]

We examined the enolate structures in THF in the presence of HMPA using low-temperature ^{7}Li, ^{31}P, and ^{13}C NMR, by measuring characteristic chemical shifts and the ^{7}Li–^{31}P coupling constant.[5c,14] The lithium enolate **3** was found to have established the dynamic equilibrium in ethereal solvents illustrated in Scheme 2. According to this Scheme, for both the tetramer **T** and the dimer **D**, the first subfix represents the number of attached HMPAs and the second subfix denotes the number of coordinated THF ligands.[18] The equilibrium point is thermodynamically determined by the enolate concentration and the quantity of HMPA. In the presence of excess HMPA, the enolate largely exists as a bis-HMPA coordinated dimer $\mathbf{D_{2,2}}$ in THF.[19,20] Tetramers,[19,20] trimers,[5c,21] and monomers,[5c,14b] however, were not detected.

^{7}Li- and ^{31}P-NMR spectra of 0.16 M THF solutions of **3** at −100 °C[22] are shown in Fig. 1, A and B, respectively. Without HMPA, the enolate exists as a mixture of $\mathbf{T_{0,4}}$ and $\mathbf{D_{0,4}}$ in a ratio of 2:3.[17] These aggregates are in rapid equilibrium even at −100 °C, giving a broad singlet at −0.36 ppm (Fig. 1 Aa). The addition of 6 molar amounts of HMPA generated $\mathbf{D_{2,2}}$ exclusively,[23] giving a 1:1 ^{7}Li doublet at −0.37 ppm (Fig. 1 Ah)[22] and a 1:1:1:1 ^{31}P quartet at 25.9 ppm (Fig. 1 Bh) with the same coupling constant $^{2}J(^{7}\text{Li}–^{31}\text{P}) = {}^{2}J(^{31}\text{P}–^{7}\text{Li}) = 9.5$ Hz.

By careful monitoring the change of intensity of quartet signals in ^{31}P NMR as a function of added HMPA, we were able to analyze transient and terminated enolate structures. Upon addition of 0.25 molar amount of HMPA (Fig. 1 Bb), the ^{31}P quartet due to $\mathbf{D_{1,3}}$ appeared at 26.1 ppm, with $^{2}J(^{31}\text{P}–^{7}\text{Li}) = 10.3$ Hz. When >0.5 molar amount of HMPA were added, a ^{31}P quartet signal assignable to $\mathbf{D_{2,2}}$ was observed at 25.9–26.0 ppm with $^{2}J(^{31}\text{P}–^{7}\text{Li}) = 9.5$ Hz. Addition of 2 molar amounts of HMPA reversed the relative ratio of $\mathbf{D_{1,3}}$ and $\mathbf{D_{2,2}}$ (Fig. 1 Bf), and the addition of 6 molar amounts of HMPA generated $\mathbf{D_{2,2}}$ exclusively (Fig. 1 Bh). Thus the tetramer/dimer equilibrium in the absence of HMPA is shifted to a dimeric structure by the coordination of HMPA, establishing the $\mathbf{D_{1,3}}/\mathbf{D_{2,2}}$ equilibrium. This is further supported by the appearance of free HMPA as a broad singlet at 26.1 ppm after the addition of 0.75 and 1.0 molar amounts of HMPA and the convergence on $\mathbf{D_{2,2}}$ by increasing amounts of HMPA.

The profiles of the HMPA titration in THF were also quantitatively determined (Fig. 2), by calculating the relative amounts of each enolate species and plotting them based on the ^{31}P signal intensities of $\mathbf{D_{1,3}}$, $\mathbf{D_{2,2}}$ and free HMPA observed in Fig. 1B (for the details of the calculation, see the Experimental Section). The HMPA-free enolate species are initially replaced by $\mathbf{D_{1,3}}$ and subsequently by $\mathbf{D_{2,2}}$. Here, the $\mathbf{D_{1,3}}/\mathbf{D_{2,2}}$ equilibrium is controlled by the higher coordination ability of HMPA to lithium than THF by approximately 100 times.[24]

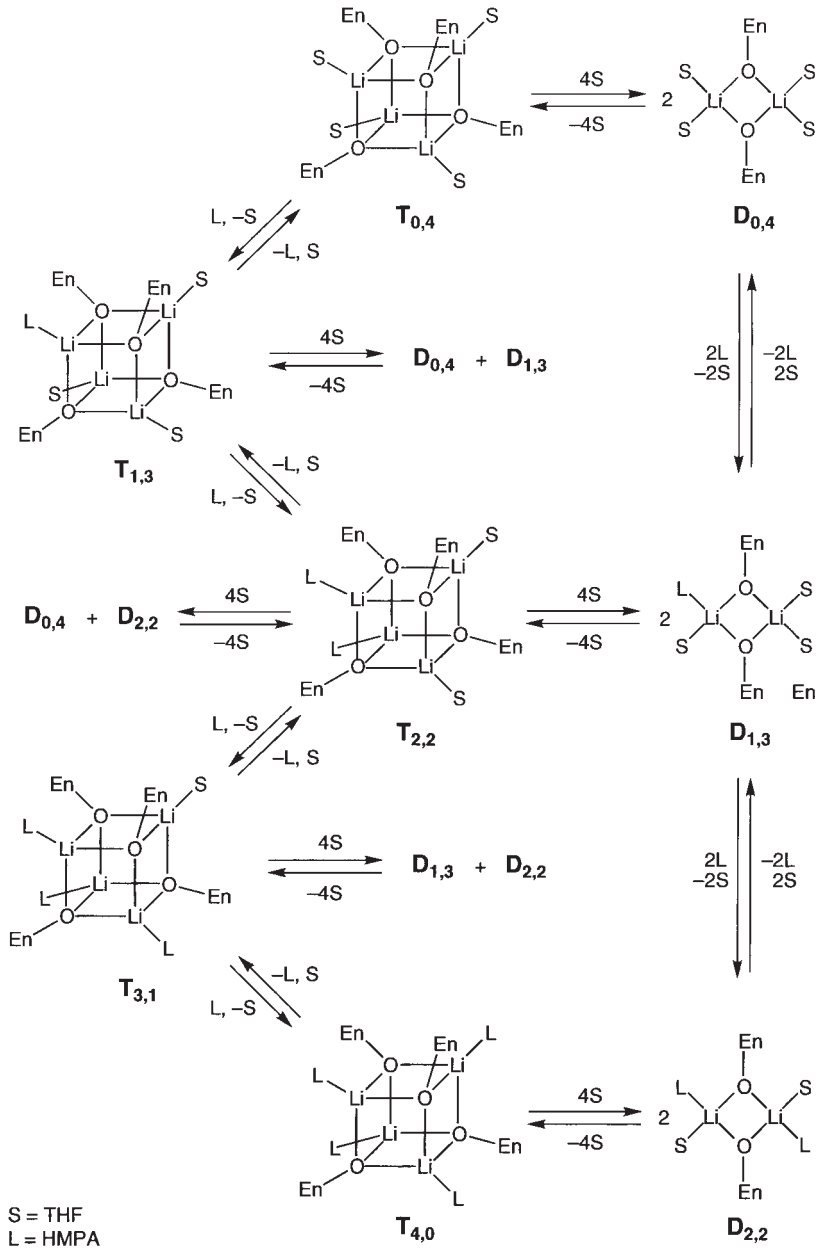

Scheme 2. Equilibrium of cyclopentanone lithium enolate in the presence of HMPA.

The monomers were undetectable in both ^{7}Li and ^{31}P spectra. Even at an enolate concentration as low as 0.04 M, or at as high as 8 molar amounts of HMPA, no high-field broad singlets arising from rapid exchange with free HMPA,[5c,14] or quintets in the −0.8 to −0.4 ppm region due to ion-paired species, were observed in ^{7}Li NMR.[5c,14] In addition, the profile of the convergence on **D$_{2,2}$** in the HMPA titration of the enolate and the clear-cut structural assignment gave no indication of any tetramers[19,20] and trimers.[5c,21] The rather broad ^{7}Li and ^{31}P signals are due to the exchange processes under the experimental conditions. In fact, the ^{7}Li and ^{31}P signals observed in diethyl ether and dimethyl ether at −100 to −110 °C are much sharper than those in THF due to the slower S/L ligand exchange.[19,20] In such ethereal solvents, the HMPA-coordinated tetramers depicted in Scheme 2 were observed as minor components.[19,20] Here, the ratio of the tetra-HMPA coordinated tetramer and the corresponding bis-HMPA coordinated dimer was independent of the quantity of added HMPA, but was influenced by the enolate concentration, confirming the establishment of the equilibrium between **T$_{4,0}$** and **D$_{2,2}$** as shown in Scheme 2.[19] Further, the ratio of the corresponding tetramer and dimer changes in the order of 5:95, <1:99, and 0:100 in diethyl ether, dimethyl ether, and THF, respectively, depending on the basicity of S.[19] Thus, in more solvative THF, only the dimer **D$_{2,2}$** was observed.

Full spectral data for the cyclopentanone lithium enolate aggregates in THF are summarized in Table 1.

The convergence of the dimeric structure in the presence of excess amounts of HMPA was also confirmed by the ^{13}C-NMR signal of their oxygen-bearing carbon. Thus, the ^{13}C-NMR spectrum of THF-d_8 containing 6 molar amounts of HMPA showed only a single broad band at 169.5 ppm, indicating that

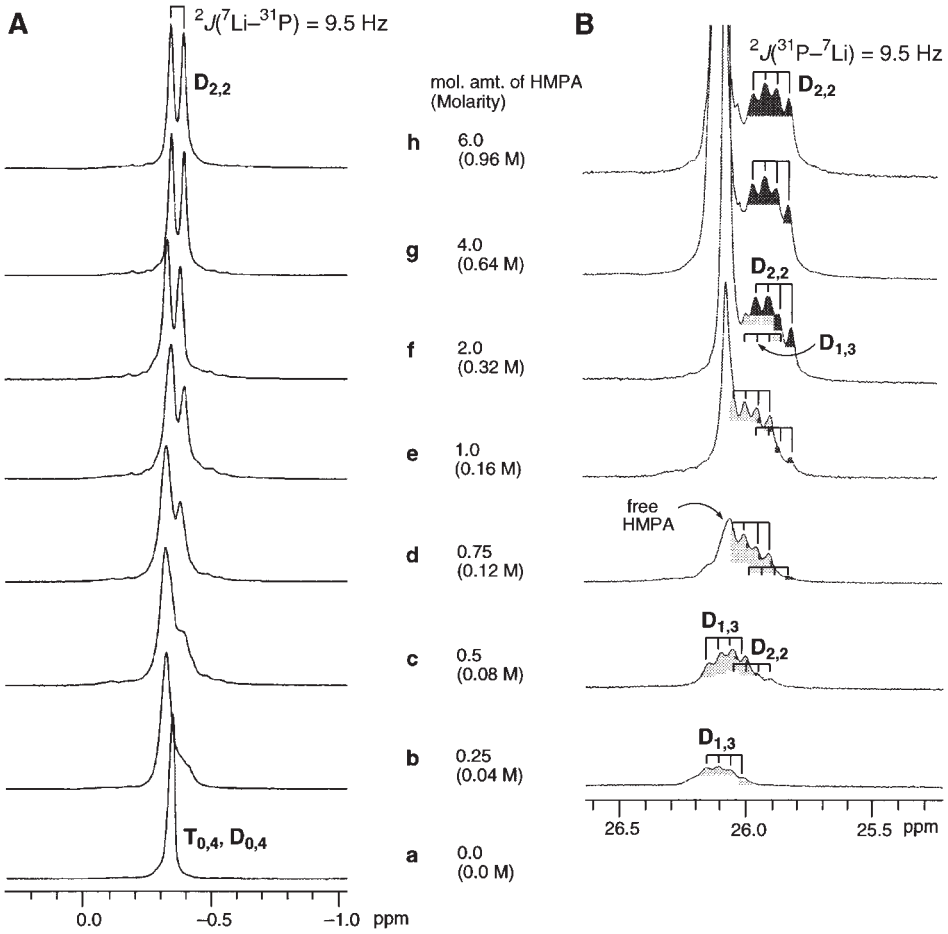

Fig. 1. HMPA titration of a 0.16 M THF solution of cyclopentanone lithium enolate **3** at −100 °C. A: ^{7}Li-NMR spectra. B: ^{31}P-NMR spectra.

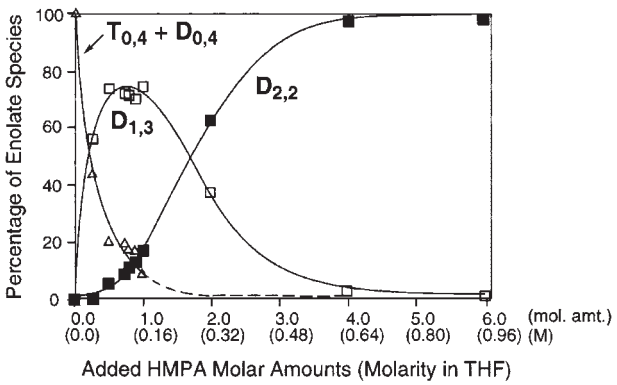

Fig. 2. The percentage of each aggregate species as functions of added HMPA for 0.16 M lithium enolate **3** in THF.

only $\mathbf{D_{2,2}}$ is formed under such a condition.

The values of ^{7}Li quadrupole-splitting constants (QSC)[25,26] for a 0.2 M THF-d_8 solution of cyclopentanone lithium enolate **3** in the presence of 5 molar amounts of HMPA[27] at 30 °C were calculated as 116 kHz, using the equation $7.5(T_1(^{13}C)/T_1(^7Li))^{1/2} \times 10^4$ (Hz), with observed ^{13}C (hydrogen-bearing vinylic carbon) and ^{7}Li spin–lattice relaxation times of 1.56 and 0.657 s, respectively. Although efforts have been made to correlate QSC values with enolate aggregate structure for some lithium enolates[5a,25,26] and phenoxides,[5b,c,25] no general rule has emerged from these attempts. For any aggregate, it is difficult to estimate the influence of a ligand solvating to Li, or of the bulkiness of the enolate anion, on QSC values.[28] Lithium 2,6-dimethylphenoxide is the only lithium enolate-related compound known to have dimeric structure in dioxolane, THF, and pyridine, with QSC values of 147, 169, and 116 kHz, respectively.[5b] Since the dimeric structure of the cyclopentanone lithium enolate $\mathbf{D_{2,2}}$ was deduced unambiguously by the HMPA titration, the QSC value obtained in this study is the first for the lithium enolate with a dimeric structure.

In summary, cyclopentanone lithium enolate **3** in THF (0.04–0.2 M) undergoes successive S/L ligand exchanges by increasing HMPA to form $\mathbf{D_{1,3}}$ and $\mathbf{D_{2,2}}$, and eventually converges on the bis-HMPA coordinated dimer $\mathbf{D_{2,2}}$ with excess HMPA.[29]

Kinetics of Alkylation of the Lithium Enolate. (a) Effects of HMPA on Rates: The reactivity and selectivity of the methylation of enolates are markedly influenced by the HMPA addend. In THF, enolate **3** was reacted slowly with methyl iodide at temperatures below −50 °C. Addition of 0.64 M HMPA enhanced the rate of methylation of a 0.06 M solution of **3** by a factor of 7500 ($(-d[CH_3I]/dt)/[CH_3I] = 8.67 \times 10^{-8}$ s^{-1} vs

Table 1. ^{7}Li and ^{31}P Chemical Shifts and Coupling Constants for the HMPA Solvated Dimer of Cyclopentanone Lithium Enolate in THF[a)]

mol. amt. of HMPA	^{7}Li (s[b)]) δ[c)]	^{7}Li (d[b)]) δ[c)] ($^{2}J(^{7}\mathrm{Li}-^{31}\mathrm{P})$[d)])	
	D$_{1,3}$	**D$_{1,3}$**	**D$_{2,2}$**
0.25		f	
0.5		f	
0.75	−0.32[e)]	−0.36[g)] (10.7)	
1.0	−0.34[e)]	−0.37[g)] (10.5)	
2.0	−0.30[e)]	−0.36[g)] (10.1)	
4.0			−0.37 (9.5)
6.0			−0.37 (9.5)
		^{31}P (q[b)]) δ[c)] ($^{2}J(^{31}\mathrm{P}-^{7}\mathrm{Li})$[d)])	
		D$_{1,3}$	**D$_{2,2}$**
0.25		26.1 (10.3)	
0.5		26.1 (10.3)	26.0 (9.5)
0.75		26.0 (10.3)	25.9 (9.5)
1.0		26.0 (10.3)	25.9 (9.5)
2.0		26.0 (10.3)	25.9 (9.5)
4.0			25.9 (9.5)
6.0			25.9 (9.5)

a) Spectra were recorded at −100 °C. b) s = singlet, d = doublet, and q = quartet. c) The chemical shifts are reported relative to external standard as described in the Experimental Section. d) All coupling constants J are reported in hertz. e) The signal was superimposed on the lower field peak of doublet due to HMPA-coordinated Li. f) Unassignable broad signal. g) The signal involves HMPA-coordinated Li atoms in both **D$_{1,3}$** and **D$_{2,2}$**.

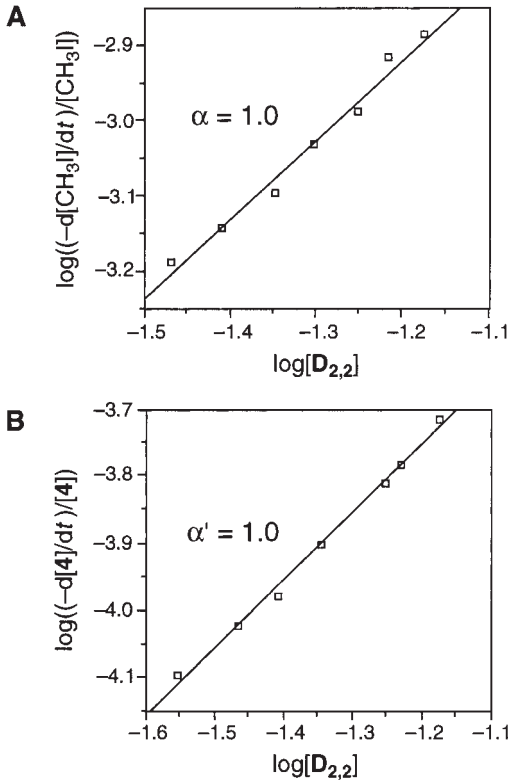

Fig. 3. Log–log plots of initial rates/[CH_3I] and initial rates/[**4**] as a function of the concentrations of the dimeric lithium enolate **D$_{2,2}$** in THF for alkylation (A) and proton abstraction reaction (B), in the presence of a fixed concentration of HMPA. The α (α') values derived from the slopes were 1.0 for both reactions.

6.53×10^{-4} s^{-1} at −75 °C).[30] In contrast, the same concentration of HMPA accelerated proton abstraction from 2-methylcyclopentanone (**4**), resulting in polymethylation, by only a factor of five ($(-\mathrm{d}[\mathbf{4}]/\mathrm{d}t)/[\mathbf{4}] = 1.80 \times 10^{-5}$ s^{-1} vs 9.46×10^{-5} s^{-1} at −50 °C). These combined effects of HMPA resulted in significantly increased selectivity of monomethylation.[6c]

(b) Aggregation State of the Reacting Enolate: We used enolate **3** concentrations of 0.06 to 0.13 M, and HMPA concentrations of 0.36 to 0.64 M, in THF. Under these concentrations, **3** exists only as a bis-HMPA coordinated dimer **D$_{2,2}$**. Since concentrations of the other aggregates in the equilibrium (Scheme 2) are negligible, the rates for the alkylation and proton abstraction reactions are simplified to Eqs. 1 and 2, respectively.[2]

$$-\mathrm{d}[\mathrm{CH_3I}]/\mathrm{d}t = k_{\mathrm{R}}[\mathbf{D_{2,2}}]^{\alpha}([\mathrm{HMPA}] - 2[\mathbf{D_{2,2}}])^{p}[\mathrm{CH_3I}] \quad (1)$$

$$-\mathrm{d}[\mathbf{4}]/\mathrm{d}t = k_{\mathrm{H}}[\mathbf{D_{2,2}}]^{\alpha'}([\mathrm{HMPA}] - 2[\mathbf{D_{2,2}}])^{p'}[\mathbf{4}] \quad (2)$$

The superscript α (or α') is the reaction order, which is equal to n_k/n_a, where n_a is the average equilibrium aggregation number and n_k is the average kinetic aggregation number.[2b,c] The superscript p (or p') is the number of free HMPA molecules that modulate the reaction of the aggregate.[31]

The reaction orders (α and α') can be determined on the basis of the reaction rates and the concentrations of the dominant dimer. The reaction conditions were chosen to be consistent with the structural study, as well as to minimize any unnecessary side reactions such as polyalkylation and the aldol reaction. Thus alkylation was carried out using 0.034–0.067 M of **D$_{2,2}$** in THF at −75 °C under pseudo-first-order conditions, with constant concentrations of CH_3I (8 mM) and HMPA (0.64 M). The rate was determined within 10% conversion after rapid quenching of the unreacted **D$_{2,2}$** with chlorotrimethylsilane. Similarly, the proton exchange rate between **D$_{2,2}$** (0.028–0.067 M) and the methyl ketone **4** (10 mM) in THF at −50 °C[32] was determined by monitoring the consumption of **4** by rapid silylation of the enolates or the formation of the enolate of **4**. Consequently, the α and α' values were determined to be 1.0 for both the alkylation and proton abstraction reactions from the slopes shown in Fig. 3, indicating that the average kinetic aggregation number for each reaction is 2.0. These findings indicate that the dimeric enolate is responsible for both reactions. This result also eliminates the possibility that undetected, but highly reactive monomeric enolate species, participate in these reactions.[2] This conclusion is in contrast to that of Streitwieser's work on different Li enolates, clarifying that (1) the monomeric enolates are responsible for alkylation,[2b,c,e,f] and (2) proton exchange is promoted by both the monomeric and dimeric enolates.[2d]

(c) Kinetic Roles of HMPA in Alkylation and Proton Abstraction: Rate studies in the presence of HMPA revealed that free HMPA molecules behave differently during the methylation[2e] and proton abstraction reactions.[31]

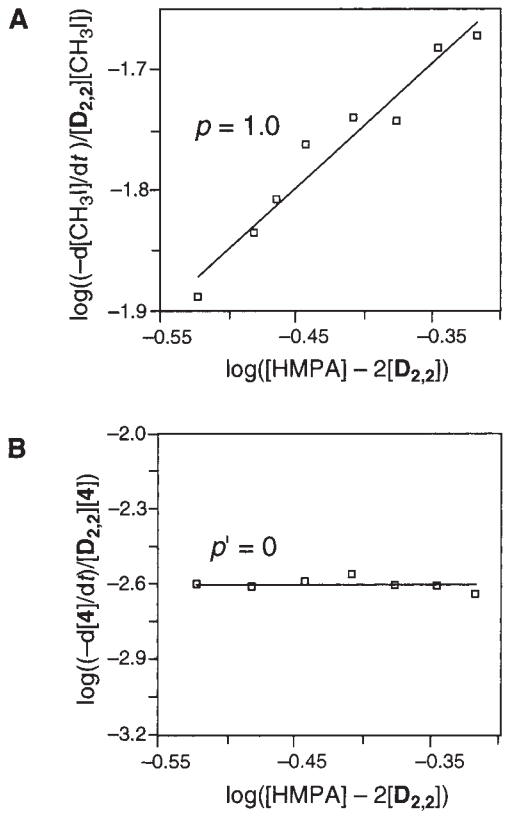

Fig. 4. HMPA dependence of the rates of alkylation (A) and proton abstraction reaction (B) in THF. The slopes, which correspond to the reaction order, indicate that one molecule of HMPA participates in the alkylation, while the proton abstraction rates are independent of HMPA concentration.

The alkylation reaction conducted in THF in the presence of 6–9 molar amounts of HMPA (0.36–0.54 M), with the constant concentrations of $\mathbf{D_{2,2}}$ (0.03 M) and CH_3I (8 mM). A plot of $\log((-d[CH_3I]/dt)/[\mathbf{D_{2,2}}][CH_3I])$ vs $\log([HMPA] - 2[\mathbf{D_{2,2}}])$ gave approximate first-order behavior for free HMPA (Fig. 4A). Thus, the alkylation rate was calculated from Eq. 3.

$$-d[CH_3I]/dt = k_R[\mathbf{D_{2,2}}]([HMPA] - 2[\mathbf{D_{2,2}}])[CH_3I] \quad (3)$$

The observed initial rate is increased consistently by the increase of HMPA addend at HMPA concentrations more than 0.36 M (Fig. 5), where only $\mathbf{D_{2,2}}$ is observed by NMR (Fig. 1).[33] The resulting linear correlation is expressed by 1.35×10^{-2} $M^{-1}\,s^{-1}$ + 4.54×10^{-2} $M^{-2}\,s^{-1}$ ([HMPA] − 0.36 M), indicating that the initial rate constant at 0.36 M HMPA is 1.35×10^{-2} $M^{-1}\,s^{-1}$ and the third-order rate constant (k_R) is 4.54×10^{-2} $M^{-2}\,s^{-1}$ (−75 °C) at 0.03 M $\mathbf{D_{2,2}}$ and 8 mM CH_3I. Thus, we concluded that an additional HMPA molecule is involved in the methylation of $\mathbf{D_{2,2}}$ at HMPA concentration higher than 0.36 M.

In contrast, the rate of proton abstraction of **4** (10 mM) in THF was independent of HMPA concentration (0.36–0.54 M) (Fig. 4B). Thus the rate of this reaction is expressed by Eq. 4 in the same range of the HMPA concentration (>0.36 M) as alkylation.

$$-d[\mathbf{4}]/dt = k_H[\mathbf{D_{2,2}}][\mathbf{4}] \quad (4)$$

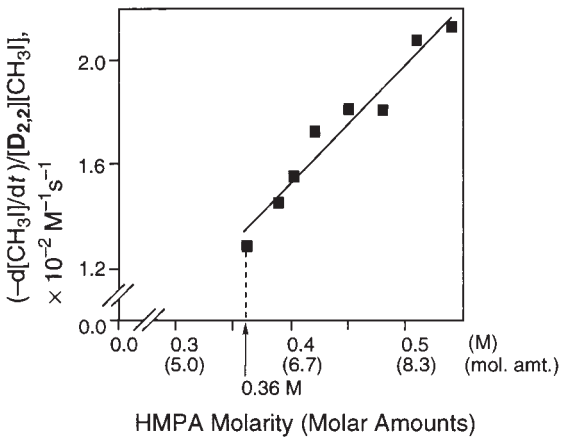

Fig. 5. Plots of the initial rates of alkylation in THF against HMPA concentrations. The line equation is expressed by $\text{rate}/[\mathbf{D_{2,2}}][CH_3I] = 1.35 \times 10^{-2}$ $M^{-1}\,s^{-1}$ + 4.54×10^{-2} $M^{-2}\,s^{-1}$ ([HMPA] − 0.36 M) at 0.03 M $\mathbf{D_{2,2}}$ and 8 mM CH_3I.

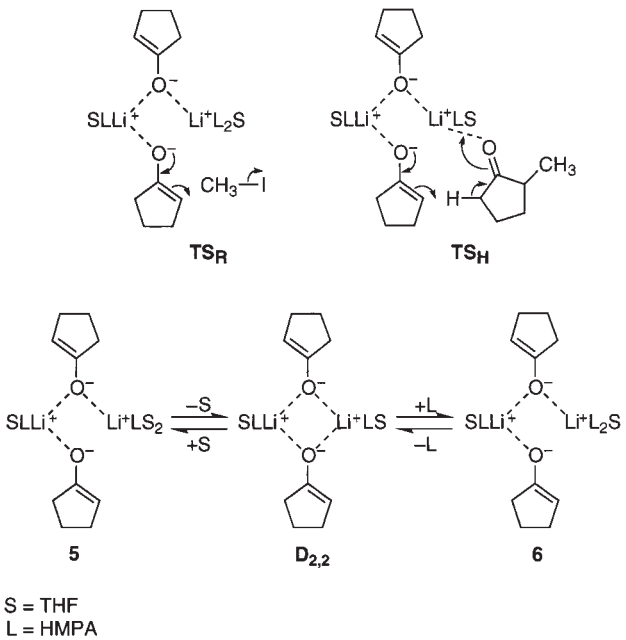

Scheme 3. Possible transition state structures for alkylation and proton abstraction reactions.

This yielded a second-order rate constant, $k_H = 2.54 \times 10^{-3}$ $M^{-1}\,s^{-1}$, at −50 °C.[32]

These results indicate that both the methylation and proton exchange reactions of **3** involve the dimeric enolate, but that the number of HMPA molecules involved in the transition structures is different. This rate-law difference explains the kinetic role of HMPA in altering the selectivity of monoalkylation.[1,6c]

Possible Transition Structures. Various transition states are conceivable for reactions of the lithium enolate **3**. The foregoing structural and rate studies urge us to propose the transition state structures, $\mathbf{TS_R}$ and $\mathbf{TS_H}$, for the alkylation and proton abstraction reactions, respectively (Scheme 3). The enolate dimer $\mathbf{D_{2,2}}$, which possesses a Li_2O_2 four-membered ring,

would equilibrate with the open form **5**, with the assistance of a solvent molecule or a ketonic substrate. The Li/O=C association in **5** (S = ketone or solvent) would thus enhance the acidity of the carbonyl α proton, and, at the same time, would increase the basicity of the enolate moiety. As a consequence, proton abstraction would take place via the cyclic transition structure $\mathbf{TS_H}$, involving two Li atoms.[34,35] Further, action of HMPA on $\mathbf{D_{2,2}}$ generates the open dimer **6**, which possesses a more highly polarized Li–O bond than **5**, due to the additional HMPA coordination that enhances the nucleophilicity of the enolate. The open dimer **6** would then undergo S_N2 displacement of CH_3I via $\mathbf{TS_R}$.

Conclusions

This study shows the significance of dimeric lithium enolates in organic reactions. In the presence of an excess amount of HMPA, cyclopentanone lithium enolate **3** exists as a dimer in THF. This dimer participates in alkylation with methyl iodide and proton exchange with a cyclopentanone derivative. While HMPA markedly enhances the reactivity of the enolate in alkylation, it does not affect proton exchange. This conclusion, however, is limited to the cyclopentanone enolate **3** under the above stated conditions.[29] Lithium enolates can exist in various forms, and each form has a different nucleophilicity and basicity.[3,10] The structures and reactivities of these enolates are highly dependent on their concentrations and steric and electronic properties, as well as on the additives, solvents, and temperature of reaction.

Experimental

General. All apparatus used in the reactions were dried in an oven (100 °C) overnight and baked out with a heat gun under reduced pressure to remove air and moisture, and then filled with argon (Ar) after they had cooled to room temperature. The air and moisture sensitive materials were manipulated under Ar using a glove box, vacuum line, and syringe techniques.

Solvent and Materials. THF was freshly distilled over sodium diphenylketyl. Solvents used for the NMR measurements (THF and THF-d_8) were distilled over sodium diphenylketyl, and then transferred into a receiver containing a sodium–potassium alloy and distilled under vacuum. These solvents were degassed prior to use. Hexamethylphosphoric triamide (HMPA) was obtained from Tokyo Kasei and distilled over CaH_2 under reduced pressure. 1-(Trimethylsiloxy)cyclopentene was purchased as commercial grade (97%). NMR studies were done using the enol silyl ether of 99.8% purity after distillation (bp 156 °C, 101 kPa) equipped with a Hempel-type distilling column. HMPA and the enol silyl ether were stored in ampoules under Ar. Butyllithium in hexane was purchased from Nacalai Tesque, Inc., and stored in a Schlenk tube equipped with a Young's tap under Ar at 4 °C. Diphenylacetic acid used as an indicator was recrystallized from methanol and dried at 60 °C under high vacuum. Methyl iodide obtained from Nacalai was distilled over P_4O_{10}. 2-Methylcyclopentanone obtained from Aldrich was purified by treatment with aqueous $KMnO_4$ and distilled over molecular sieves 13X. Nonane used as the internal standard for the kinetic studies was distilled over molecular sieves 3A. Chlorotrimethylsilane and triethylamine were distilled over CaH_2.

NMR Spectroscopy. All the multinuclear NMR experiments were recorded on a JEOL JNM Λ-500 spectrometer operated at 194.25 MHz (^{7}Li), 202.35 MHz (^{31}P), or 125.65 MHz (^{13}C). The ^{7}Li and ^{31}P chemical shifts were referenced to external standards, 0.41 M LiCl/THF-d_8 (δ 0.0) and 1.0 M $P(C_6H_5)_3$/THF-d_8 (δ −6.0), respectively, at −100 °C. Shiming was performed on the external reference at −100 °C and ^{7}Li- and ^{31}P-NMR spectra were then taken without locking. The ^{13}C chemical shifts were referenced to tetramethylsilane/THF-d_8 (δ 0.0) as an external standard at −100 °C. Digital resolutions were 0.59, 0.79, and 0.23 Hz for ^{7}Li, ^{31}P, and ^{13}C, respectively.

The ^{7}Li and ^{13}C relaxation times ($T_1(^7\text{Li})$ and $T_1(^{13}\text{C})$) were measured with the inversion-recovery method, and data were processed by nonlinear least-squares programs.

Product Analysis. Gas chromatographical (GC) analyses were performed on a Shimadzu GC-14B instrument with a flame ionization (FID) and a capillary column (TC-1, 0.25 mm × 60 m, Shimadzu Inc.); carrier gas, N_2 (pressure of 0.5 kg/cm^2); split ratio, 30:1; initial column temperature, 70 °C for 8 min; final column temp., 250 °C; progress rate, 20 °C/min; detection temp., 280 °C; retention time (t_R) of cyclopentanone, 8.5 min; t_R of 2-methylcyclopentanone, 11.7 min; t_R of 1-(trimethylsiloxy)cyclopentene, 15.2 min.

General Procedure for Preparation of Cyclopentanone Lithium Enolate. 1-(Trimethylsiloxy)cyclopentene (78.2 mg, 0.500 mmol) was placed into a 10-mL test tube with positive Ar pressure. THF (1.5 mL) was added, and then the solution was transferred through a stainless cannula into a 20-mL Schlenk tube. To the solution was added butyllithium (1.43 M hexane solution, 0.344 mL, 0.500 mmol) at 0 °C via a syringe under Ar purge. The mixture was left to stand at room temperature for 1.0 h under Ar atmosphere.

Preparation of Samples for ^{7}Li and ^{31}P NMR Spectroscopic Analyses (Fig. 1). A THF solution of the lithium enolate was prepared as described above. The solution was cooled to 0 °C with an ice bath, and 0.25 molar amount of HMPA (22.4 mg, 0.125 mmol) was added, followed by additional THF to give a total volume of 3.1 mL. A 5-mm NMR tube was charged with this solution (750 μL); the filled tube was cooled to 77 K and then sealed with a flame under vacuum. Samples to which 0.50, 0.75, 1.0, 2.0, 4.0, and 6.0 molar amounts of HMPA were added were prepared according to this procedure. NMR samples were kept at −80 °C. Spectral confidence was confirmed by repreating the same preparation procedure. NMR samples were kept at −80 °C and quickly used for the NMR measurement. The solutions of some samples changed from colorless to yellow after one week and were contaminated by several undesirable peaks as judged by ^{7}Li NMR.

Procedure to Deduce the Percentage of HMPA-Free Aggregates, Mono- and Bis-HMPA Coordinated Dimers (Fig. 2). When a molar amount of HMPA is added, the relation between the total quantity of HMPA molecules ($\langle\text{HMPA}\rangle_{\text{total}}$) and the total quantity of Li atoms ($\langle\text{Li}\rangle_{\text{total}}$) is given by Eq. 5:

$$\langle\text{HMPA}\rangle_{\text{total}} = a\langle\text{Li}\rangle_{\text{total}} \tag{5}$$

In the presence of HMPA, cyclopentanone lithium enolate exists as a mixture of HMPA-free aggregates ($(\text{LiOEn})_n$), $\mathbf{D_{1,3}}$, and $\mathbf{D_{2,2}}$. In this case, the total quantity of Li atoms is expressed as Eq. 6:

$$\begin{aligned}\langle\text{Li}\rangle_{\text{total}} &= \Sigma n[(\text{LiOEn})_n] + 2[\mathbf{D_{1,3}}] + 2[\mathbf{D_{2,2}}] \quad (n = 1,\ 2,\ \ldots)\\ &= \{\text{LiOEn}\} + 2[\mathbf{D_{1,3}}] + 2[\mathbf{D_{2,2}}]\end{aligned} \tag{6}$$

where {LiOEn} means the formal concentration of HMPA-free enolate. Likely, the total quantity of HMPA molecules is given by the sum of the quantity of free and coordinated HMPA.

$$\langle \mathrm{HMPA} \rangle_{\mathrm{total}} = [\mathrm{HMPA}] + [\mathbf{D_{1,3}}] + 2[\mathbf{D_{2,2}}] \quad (7)$$

The following value p, which is obtained by the ratio of intensities of two ^{31}P quartet signals, corresponds to the relative quantity of the coordinated HMPA for $\mathbf{D_{1,3}}$ and $\mathbf{D_{2,2}}$ (Fig. 1B).

$$p = 2[\mathbf{D_{2,2}}]/[\mathbf{D_{1,3}}]$$

The value q, which is obtained by the integral ratio of a singlet and two quartet signals, corresponds to the relative quantity between free and coordinated HMPA.

$$q = [\mathrm{HMPA}]/([\mathbf{D_{1,3}}] + 2[\mathbf{D_{2,2}}])$$

From Eqs. 5–7, p and q, the relative concentration between {LiOEn} and $[\mathbf{D_{1,3}}]$ is derived (Eq. 8).

$$\{\mathrm{LiOEn}\}/[\mathbf{D_{1,3}}] = (p+1)(q+1)/a - (p+2) \quad (8)$$

Thus, the relative concentrations between $\mathbf{D_{1,3}}$ and $\mathbf{D_{2,2}}$ and between HMPA-free LiOEn and $\mathbf{D_{1,3}}$ are determined from $p/2$ and $(p+1)(q+1)/a - (p+2)$, respectively.

The numbers A, B, and C, are the proportions of {LiOEn}, $[\mathbf{D_{1,3}}]$, and $[\mathbf{D_{2,2}}]$, respectively, and are calculated by the following Eqs. 9–11.

$$\begin{aligned} \mathrm{A} &= \{\mathrm{LiOEn}\}/(\{\mathrm{LiOEn}\} + [\mathbf{D_{1,3}}] + [\mathbf{D_{2,2}}]) \\ &= \{(p+1)(q+1)/a - (p+2)\} \\ &\quad /\{(p+1)(q+1)/a - (p+2)/2\} \end{aligned} \quad (9)$$

$$\begin{aligned} \mathrm{B} &= [\mathbf{D_{1,3}}]/(\{\mathrm{LiOEn}\} + [\mathbf{D_{1,3}}] + [\mathbf{D_{2,2}}]) \\ &= 1/\{(p+1)(q+1)/a - (p+2)/2\} \end{aligned} \quad (10)$$

$$\begin{aligned} \mathrm{C} &= [\mathbf{D_{2,2}}]/(\{\mathrm{LiOEn}\} + [\mathbf{D_{1,3}}] + [\mathbf{D_{2,2}}]) \\ &= p/2/\{(p+1)(q+1)/a - (p+2)/2\} \end{aligned} \quad (11)$$

Actually, the 0.16 M solution of the lithium enolate is submitted for NMR analysis and therefore, Eq. 12 is established under such condition.

$$0.16\ \mathrm{M} = \{\mathrm{LiOEn}\} + 2[\mathbf{D_{1,3}}] + 2[\mathbf{D_{2,2}}] \quad (12)$$

which is rewritten by Eq. 13.

$$[\mathbf{D_{1,3}}] + [\mathbf{D_{2,2}}] = (0.16\ \mathrm{M} - \{\mathrm{LiOEn}\})/2 \quad (13)$$

Substitution of Eq. 13 into Eq. 9 gives Eq. 14 in which the formal concentration of HMPA-free enolate in expressed with the defined number A.

$$\{\mathrm{LiOEn}\} = 0.16\mathrm{A}/(2 - \mathrm{A}) \quad (14)$$

The cyclopentanone lithium enolate is known to exist as a mixture of the tetramer $\mathbf{T_{0,4}}$ and dimer $\mathbf{D_{0,4}}$ in THF.[16] Assuming that the equilibrium constant for the HMPA-free enolate, $K = [\mathbf{D_{0,4}}]^2/[\mathbf{T_{0,4}}]$, could be adapted in a range of our enolate concentrations, each concentration of HMPA-free aggregates, $\mathbf{T_{0,4}}$ and $\mathbf{D_{0,4}}$, at a given enolate concentration is determined using K ($= 0.15 \pm 0.02$ M) deduced from the melting point depression in THF.[16] Here, an average aggregation number ($n_a, n_a = \Sigma n^2[(\mathrm{LiOEn})_n]/\Sigma n[(\mathrm{LiOEn})_n]$) is given by Eq. 15.

$$n_a = (4 \times 4[\mathbf{T_{0,4}}] + 2 \times 2[\mathbf{D_{0,4}}])/(4[\mathbf{T_{0,4}}] + 2[\mathbf{D_{0,4}}]) \quad (15)$$

Thus, the actual concentration of HMPA-free aggregates is written by $\{\mathrm{LiOEn}\}/n_a$, then its proportion is A/n_a. According to the above procedure, the relative amounts (%) of HMPA-free aggregates ($\mathbf{T_{0,4}}$ and $\mathbf{D_{0,4}}$), $\mathbf{D_{1,3}}$, and $\mathbf{D_{2,2}}$ are determined by $\mathrm{A}/n_a/(\mathrm{A}/n_a + \mathrm{B} + \mathrm{C}) \times 100$, $\mathrm{B}/(\mathrm{A}/n_a + \mathrm{B} + \mathrm{C}) \times 100$, and $\mathrm{C}/(\mathrm{A}/n_a + \mathrm{B} + \mathrm{C}) \times 100$, respectively. Thus, the calculated p and q values and resulting relative amounts of $\mathbf{T_{0,4}}$, $\mathbf{D_{0,4}}$, $\mathbf{D_{1,3}}$, and $\mathbf{D_{2,2}}$ are summarized in Table 2. Overall, the percentages of the enolate species are plotted as functions of HMPA concentrations, as shown in Fig. 2.

Table 2. Calculated p and q Values and Percentages of Enolate Aggregates in THF

mol. amt. of HMPA (a)	p[a)]	q	$\mathbf{T_{0,4}}$ and $\mathbf{D_{0,4}}$	$\mathbf{D_{1,3}}$	$\mathbf{D_{2,2}}$
			%	%	%
0.25	0.00[b)]	0.00[b)]	44	56	0
0.50	0.16[b)]	0.10[b)]	20	74	6
0.75	0.26	0.71	19	71	10
0.80	0.33	0.74	17	71	12
0.90	0.38	0.91	17	70	13
1.0	0.46	0.93	9	74	17
2.0	3.3	—	0[c)]	37	63
4.0	78	—	0[c)]	3	97
6.0	98	—	0[c)]	2	98

a) Determined based on the relative intensities of right-side signals in quartets. b) In a range of added HMPA quantity less than 0.5 mol. amt., the quantity of free HMPA cannot be estimated directly because of its signal superimposition on that of coordinated HMPA. Therefore, the p and q values were determined according to Eqs. 9–11 based on A/n_a, B, and C values obtained by the extrapolation of the defined curve in a range of 0.75–1.0 mol. amt. of added HMPA. c) The enolate percentages are calculated by assuming that HMPA-free enolate would be absent in these HMPA quantities.

General Procedure for Kinetic Studies. (a) Determination of the Reaction Order of the Lithium Enolate for Alkylation (Fig. 3A): The lithium enolate was prepared in THF as described above. To the resulting solution, HMPA (573 mg, 3.2 mmol) was added, followed by additional THF to give a total volume of 5.0 mL. After the solution was left to stand at room temperature for 1.0 h, the solution was cooled in a CryoCool-controlled −75 °C bath. Aliquots of a stock THF solution of methyl iodide (0.4 M, 0.10 mL, 0.04 mmol) containing nonane as GC standard (7.18 mg, 0.056 mmol) were added via a syringe. After the mixture had been stirred for 1.0 min, chlorotrimethylsilane (514 mg, 4.7 mmol) and triethylamine (479 mg, 4.7 mmol) were added, and then a saturated aqueous $NaHCO_3$ solution (1 mL) was poured into the solution. The organic layer was separated and the aqueous layer was extracted twice with ether (2 mL). The combined organic solutions were dried over Na_2SO_4. The reaction mixtures were submitted to GC analysis. The reactions for 1.5, 2.0, and 2.5 min were repeated by a similar procedure. The initial rates were measured based on the yield of 2-methylcyclopentanone. Kinetic studies were carried out with the change of the concentration of the lithium enolate from 0.07 to 0.13 M as described above. The resulting rates are summarized in Table 3. The plotting in Fig. 3A was conducted based on these kinetic data.

(b) Determination of the Reaction Order of the Lithium Enolate for Proton Abstraction Reaction (Fig. 3B): The lithium enolate was prepared in THF as described above. To the solution was added HMPA (573.4 mg, 3.2 mmol) and this was followed by additional THF to give a total volume of 5.0 mL. After the solution was left to stand at room temperature for 1.0 h, the solution was cooled in a CryoCool-controlled −50 °C bath. A 0.5 M THF solution of 2-methylcyclopentanone (0.10 mL, 0.05 mmol)

Table 3. Initial Rates of Alkylation at Several Concentrations

[$\mathbf{D_{2,2}}$]/M	x[a)]	$(-d[CH_3I]/dt)/[CH_3I]$ (s^{-1})	y[b)]
0.034	−1.47	6.52×10^{-4}	−3.19
0.039	−1.41	7.16×10^{-4}	−3.14
0.045	−1.35	7.96×10^{-4}	−3.10
0.050	−1.30	9.27×10^{-4}	−3.03
0.056	−1.25	1.03×10^{-3}	−2.30
0.061	−1.21	1.21×10^{-3}	−2.92
0.067	−1.17	1.30×10^{-3}	−2.88

a) x: log[$\mathbf{D_{2,2}}$]. b) y: log((−d[CH_3I]/dt)/[CH_3I]).

Table 4. Initial Rates of Proton Abstraction at Several Concentrations

[$\mathbf{D_{2,2}}$]/M	x[a)]	$(-d[\mathbf{4}]/dt)/[\mathbf{4}]$ (s^{-1})	y[b)]
0.028	−1.55	7.97×10^{-5}	−4.10
0.034	−1.47	9.46×10^{-5}	−4.02
0.039	−1.41	1.05×10^{-4}	−3.98
0.045	−1.35	1.25×10^{-4}	−3.90
0.056	−1.25	1.55×10^{-4}	−3.81
0.059	−1.23	1.65×10^{-4}	−3.78
0.067	−1.17	1.92×10^{-4}	−3.72

a) x: log[$\mathbf{D_{2,2}}$]. b) y: log((−d[**4**]/dt)/[**4**]).

containing nonane as GC standard (7.18 mg, 0.056 mmol) was added via a syringe. After the mixture had been stirred for 4.0 min, chlorotrimethylsilane (1.37 g, 13.0 mmol) and triethylamine (1.28 g, 13.0 mmol) were added, and then saturated aqueous $NaHCO_3$ solution (1 mL) was poured into the mixture. The organic layer was separated, and the aqueous layer was extracted twice with ether (2 mL). The combined organic extracts were submitted to GC analysis. The reactions for 8.0 and 12.0 min were repeated by a similar procedure. Initial rates were measured based on the yield of 2-methylcyclopentanone. Kinetic studies were carried out with the change of the concentration of the lithium enolate from 0.06 to 0.13 M as described above. The resulting rates are summarized in Table 4. The plotting in Fig. 3B was conducted based on these kinetic data.

(c) Determination of the Reaction Order of HMPA for Alkylation (Fig. 4A): The lithium enolate (0.3 mmol, 27.0 mg) was prepared in THF (1.5 mL) as described above. To the resulting solution was added HMPA (322 mg, 1.8 mmol), and followed by additional THF to give a total volume of 5.0 mL. After the solution was left to stand at room temperature for 1.0 h, the solution was cooled in a CryoCool-controlled −75 °C bath. A 0.4 M THF solution of methyl iodide (0.10 mL, 0.04 mmol) containing nonane as GC standard (7.18 mg, 0.056 mmol) was added via a syringe. After the mixture had been stirred for 5.0 min, chlorotrimethylsilane (514 mg, 4.7 mmol) and triethylamine (479 mg, 4.7 mmol) were added, and then a saturated aqueous $NaHCO_3$ solution (1 mL) was poured into the mixture. The organic layer was separated, and the aqueous layer was extracted twice with ether (2 mL). The combined organic extracts were analyzed by GC. The reactions for 10.0 and 15.0 min were repeated by the same procedure. Initial rates were measured based on the yield of 2-methylcyclopentanone. Kinetic studies were carried out with the change of the concentration of HMPA from 0.36 to 0.54 M as described above. The resulting rates are summarized in Table 5. The plotting in Fig. 4A was conducted based on these kinetic data.

Table 5. Initial Rates of Alkylation at Several Concentrations

[HMPA]/M	x[a)]	$(-d[CH_3I]/dt)/[\mathbf{D_{2,2}}][CH_3I]$ ($M^{-1}\,s^{-1}$)	y[b)]
0.360	−0.523	1.29×10^{-2}	−1.89
0.390	−0.481	1.46×10^{-2}	−1.84
0.402	−0.466	1.56×10^{-2}	−1.81
0.420	−0.444	1.73×10^{-2}	−1.76
0.450	−0.409	1.82×10^{-2}	−1.74
0.480	−0.377	1.81×10^{-2}	−1.74
0.510	−0.347	2.08×10^{-2}	−1.68
0.540	−0.319	2.13×10^{-2}	−1.67

a) x: log([HMPA] − 2[$\mathbf{D_{2,2}}$]). b) y: log((−d[CH_3I]/dt)/[$\mathbf{D_{2,2}}$][CH_3I]).

Table 6. Initial Rates of Proton Abstraction at Several Concentrations

[HMPA]/M	x[a)]	$(-d[\mathbf{4}]/dt)/[\mathbf{D_{2,2}}][\mathbf{4}]$ ($M^{-1}\,s^{-1}$)	y[b)]
0.360	−0.523	2.52×10^{-3}	−2.60
0.390	−0.481	2.44×10^{-3}	−2.61
0.420	−0.444	2.58×10^{-3}	−2.59
0.450	−0.409	2.76×10^{-3}	−2.56
0.480	−0.377	2.48×10^{-3}	−2.61
0.510	−0.347	2.48×10^{-3}	−2.61
0.540	−0.319	2.30×10^{-3}	−2.64

a) x: log([HMPA] − 2[$\mathbf{D_{2,2}}$]). b) y: log((−d[**4**]/dt)/[$\mathbf{D_{2,2}}$][**4**]).

(d) Determination of the Reaction Order of HMPA for Proton Abstraction (Fig. 4B): Kinetic studies were carried out with the 0.06 M lithium enolate under the change of the concentration of HMPA from 0.36 to 0.54 M as described above. The resulting rates are summarized in Table 6. The plotting in Fig. 4B was conducted based on these kinetic data.

This work was supported in part by Grant-in-Aids for Creative Scientific Research 13NP0401 (M.S.) and 14GS0214 (R.N.) from the Japan Society for the Promotion of Science. We thank Dr. M. Kataoka for helpful guidance in NMR measurements in Nagoya University Chemical Instrument Center.

References

1 a) R. L. Augustine, "Carbon–Carbon Bond Formation," Marcel Dekker, New York (1979), Vol. 1. b) C. H. Heathcock, "Comprehensive Organic Synthesis," ed by B. M. Trost and I. Fleming, Pergamon Press, Oxford, U. K. (1991), Vol. 3. c) D. A. Evans, "Asymmetric Synthesis," ed by J. D. Morrison, Academic Press, New York (1984), Vol. 3, pp. 1–110.

2 a) A. Abbotto and A. Streitwieser, *J. Am. Chem. Soc.*, **117**, 6358 (1995). b) F. Abu-Hasanayn, M. Stratakis, and A. Streitwieser, *J. Org. Chem.*, **60**, 4688 (1995). c) A. Abbotto, S. S.-W. Leung, A. Streitwieser, and K. V. Kilway, *J. Am. Chem. Soc.*, **120**, 10807 (1998). d) A. Streitwieser and D. Z.-R. Wang, *J. Am. Chem. Soc.*, **121**, 6213 (1999). e) S. S.-W. Leung and A. Streitwieser, *J. Org. Chem.*, **64**, 3390 (1999). f) D. Z. Wang, Y.-J. Kim, and A. Streitwieser, *J. Am. Chem. Soc.*, **122**, 10754 (2000).

3 Review: D. Seebach, *Angew. Chem., Int. Ed. Engl.*, **27**,

1624 (1988).

4 R. Amstutz, W. B. Schweizer, D. Seebach, and J. D. Dunitz, *Helv. Chim. Acta*, **64**, 2617 (1981).

5 a) L. M. Jackman and N. M. Szeverenyi, *J. Am. Chem. Soc.*, **99**, 4954 (1977). b) L. M. Jackman and C. W. DeBrosse, *J. Am. Chem. Soc.*, **105**, 4177 (1983). c) L. M. Jackman and X. Chen, *J. Am. Chem. Soc.*, **114**, 403 (1992).

6 a) M. Suzuki, A. Yanagisawa, and R. Noyori, *J. Am. Chem. Soc.*, **107**, 3348 (1985). b) M. Suzuki, A. Yanagisawa, and R. Noyori, *J. Am. Chem. Soc.*, **110**, 4718 (1988). c) Y. Morita, M. Suzuki, and R. Noyori, *J. Org. Chem.*, **54**, 1785 (1989). d) M. Suzuki, Y. Morita, H. Koyano, M. Koga, and R. Noyori, *Tetrahedron*, **46**, 4809 (1990).

7 a) P. A. Tardella, *Tetrahedron Lett.*, **10**, 1117 (1969). b) H. Nishiyama, K. Sakuta, and K. Itoh, *Tetrahedron Lett.*, **25**, 223 (1984). c) H. Nishiyama, K. Sakuta, and K. Itoh, *Tetrahedron Lett.*, **25**, 2487 (1984).

8 For HMPA effects on the structures of organolithium compounds, see: a) H. J. Reich and D. P. Green, *J. Am. Chem. Soc.*, **111**, 8729 (1989). b) H. J. Reich, D. P. Green, M. A. Medina, W. S. Goldenberg, B. Ö. Gudmundsson, R. R. Dykstra, and N. H. Phillips, *J. Am. Chem. Soc.*, **120**, 7201 (1998). c) H. J. Reich and W. H. Sikorski, *J. Org. Chem.*, **64**, 14 (1999). d) W. H. Sikorski and H. J. Reich, *J. Am. Chem. Soc.*, **123**, 6527 (2001).

9 L. M. Jackman and B. C. Lange, *J. Am. Chem. Soc.*, **103**, 4494 (1981).

10 L. M. Jackman and B. D. Smith, *J. Am. Chem. Soc.*, **110**, 3829 (1988).

11 E. M. Arnett and K. D. Moe, *J. Am. Chem. Soc.*, **113**, 7288 (1991).

12 For aggregated reactants such as those proposed for aldol reactions, see: a) D. Seebach, R. Amstutz, and J. D. Dunitz, *Helv. Chim. Acta*, **64**, 2622 (1981). b) C. H. Heathcock and J. Lampe, *J. Org. Chem.*, **48**, 4330 (1983). c) P. G. Williard and M. J. Hintze, *J. Am. Chem. Soc.*, **109**, 5539 (1987). d) E. M. Arnett, F. J. Fisher, M. A. Nichols, and A. A. Ribeiro, *J. Am. Chem. Soc.*, **112**, 801 (1990).

13 D. B. Collum, *Acc. Chem. Res.*, **26**, 227 (1993).

14 a) H. J. Reich and J. P. Borst, *J. Am. Chem. Soc.*, **113**, 1835 (1991). b) H. J. Reich, J. P. Borst, R. R. Dykstra, and D. P. Green, *J. Am. Chem. Soc.*, **115**, 8728 (1993).

15 A. Streitwieser, Y.-J. Kim, and D. Z.-R. Wang, *Org. Lett.*, **3**, 2599 (2001).

16 Although the lithium enolate is often generated by the reaction of a ketonic substrate with lithium diisopropylamide in an ethereal solvent, we used an amine-free pure enolate in this study to avoid the structural complication arising from the participation of the amine ligand.

17 W. Bauer and D. Seebach, *Helv. Chim. Acta*, **67**, 1972 (1984).

18 The coordination number of lithium cation is defined as four, according to general empirical formula. This consistently simplifies the following structural analyses and discussion.

19 For the details including the formation of a mixture of tetrameric and dimeric enolates in acyclic ethereal solvents, see: M. Suzuki, H. Koyama, and R. Noyori, *Tetrahedron* (2004), in press.

20 Some of the results were reported in Abstracts; M. Suzuki, H. Koyama, and R. Noyori, "48th Symposium on Organometallic Chemistry, Japan," Kinki Chemical Society, Yokohama National University, Kanagawa, Japan (2001), pp. 114–115; M. Suzuki, H. Koyama, and R. Noyori, "50th Symposium on Organometallic Chemistry, Japan," Kinki Chemical Society, Osaka University, Osaka, Japan (2003), pp. 44–45.

21 J. L. Rutherford and D. B. Collum, *J. Am. Chem. Soc.*, **121**, 10198 (1999); J. L. Rutherford and D. B. Collum, *J. Am. Chem. Soc.*, **123**, 199 (2001).

22 A doublet signal of ^{7}Li in Fig. 1 Ah became broad singlet signal at -50 °C arising from rapid ligand exchange between THF and HMPA.

23 The spectra no longer changed with increasing HMPA (8 molar amounts).

24 The degree of coordination ability was determined by the ratio of free and coordinated HMPA in the presence of equimolar amount of HMPA. For the solvation energy, see: H. J. Reich and K. J. Kulicke, *J. Am. Chem. Soc.*, **118**, 273 (1996).

25 a) L. M. Jackman, L. M. Scarmoutzos, and C. W. DeBrosse, *J. Am. Chem. Soc.*, **109**, 5355 (1987). b) L. M. Jackman and D. Çizmeciyan, *Magn. Reson. Chem.*, **34**, 14 (1996).

26 J. Q. Wen and J. B. Grutzner, *J. Org. Chem.*, **51**, 4220 (1986).

27 $\mathbf{D_{2,2}}$ is formed exclusively under these conditions.

28 QSC values in THF for α-tetralone[25a] and acetaldehyde[26] lithium enolate with tetrameric structures are 64 and 65 kHz at 30 °C and -1 °C, respectively, while the value of tetrameric isobutyrophenone lithium enolate[5a] is 136 kHz.

29 Spectra of other lithium enolates such as *p*-phenylisobutyrophenonate,[2] pinacolonate,[4] and isobutyrophenonate,[5a] were complicated and difficult to analyze.

30 Actual alkylation reactions in the absence of HMPA were conducted at temperatures from 0 to -50 °C. Therefore, the rate at -75 °C was deduced from the equation of $8.51 - 4.94 \times 10^3/T$ obtained by the Arrhenius plot ($\ln\{(d[CH_3I]/dt)/[CH_3I]\}$ against $1/T$).

31 X. Sun and D. B. Collum, *J. Am. Chem. Soc.*, **122**, 2452 (2000).

32 The same dimer $\mathbf{D_{2,2}}$ is involved in the reaction in a wide range of temperature including -50 °C as judged by Arrhenius equation ($\ln\{(d[\mathbf{4}]/dt)/[\mathbf{4}]\} = 5.98 - 1.91 \times 10^3/T$) obtained from the reaction conducted at the range of -20 to -75 °C.[22]

33 At free HMPA concentrations lower than 0.30 M in THF, alkylation rates are not linear, due to incomplete convergence on the dimer.

34 a) E. Kaufmann, P. v. R. Schleyer, K. N. Houk, and Y.-D. Wu, *J. Am. Chem. Soc.*, **107**, 5560 (1985). b) M. P. Bernstein and D. B. Collum, *J. Am. Chem. Soc.*, **115**, 789 (1993).

35 F. E. Romesberg and D. B. Collum, *J. Am. Chem. Soc.*, **117**, 2166 (1995), and references cited therein.